Gastroenterology 2019;157:552–568

Endoplasmic Reticulum Stress-Induced Upregulation of STARD1 Promotes Acetaminophen-Induced Acute Liver Failure

Sandra Torres,[1,2,*] **Anna Baulies**,[1,2,*] Naroa Insausti-Urkia,[1,2] Cristina Alarcón-Vila,[1,2] Raquel Fucho,[1,2] Estel Solsona-Vilarrasa,[1,2] Susana Núñez,[1,2] David Robles,[1,2] Vicent Ribas,[1,2] Leslie Wakefield,[3] Markus Grompe,[3] M. Isabel Lucena,[4] Raul J. Andrade,[4] Sanda Win,[5] Tin A. Aung,[5] Neil Kaplowitz,[5] Carmen García-Ruiz,[1,2,6,§] and Jose C. Fernández-Checa[1,2,6,§]

[1]Cell Death and Proliferation, IIBB-CSIC, Barcelona, Spain; [2]Liver Unit, Hospital Cínic, IDIBAPS and CIBEREHD, Barcelona, Spain; [3]Oregon Health and Science University, Portland, Oregon; [4]Unidad de Gestión Clínica de Aparato Digestivo, Servicio de Farmacología Clínica, Instituto de Investigación Biomédica de Málaga-IBIMA, CIBEREHD, Hospital Universitario Virgen de la Victoria, Universidad de Málaga, Málaga, Spain; [5]USC Research Center for Liver Disease, USC Keck School of Medicine, Los Angeles, California; [6]USC Research Center for ALPD, Keck School of Medicine, Los Angeles, California

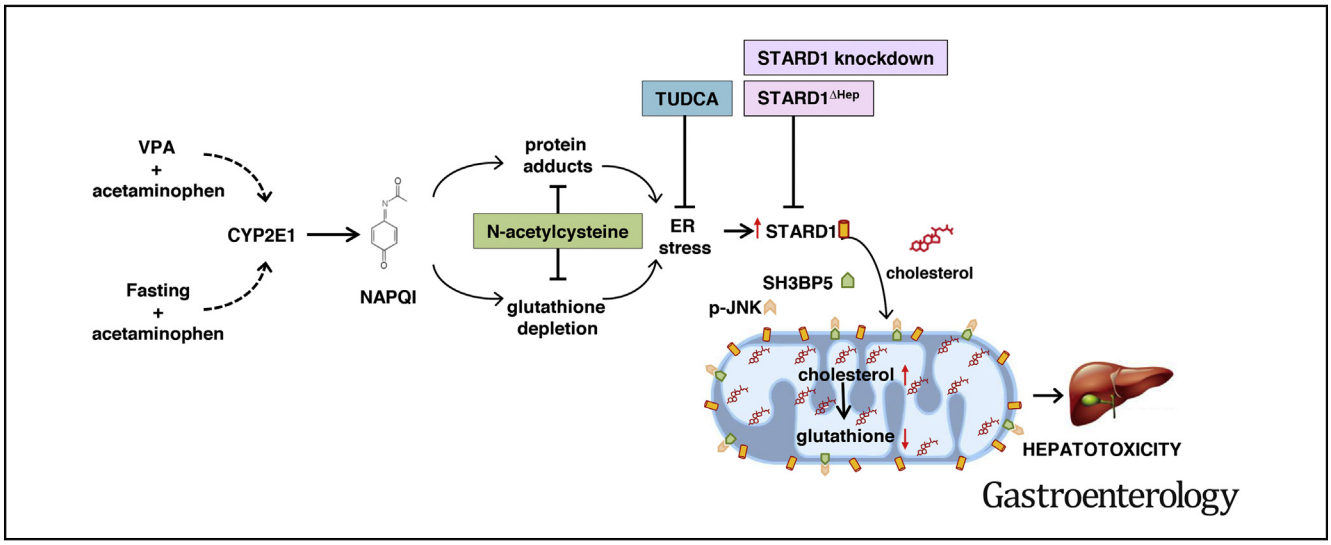

BACKGROUND & AIMS: Acetaminophen (APAP) overdose is a major cause of acute liver failure (ALF). Mitochondrial SH3BP5 (also called SAB) and phosphorylation of c-Jun N-terminal kinase (JNK) mediate the hepatotoxic effects of APAP. We investigated the involvement of steroidogenic acute regulatory protein (STARD1), a mitochondrial cholesterol transporter, in this process and sensitization by valproic acid (VPA), which depletes glutathione and stimulates steroidogenesis. **METHODS:** Nonfasted C57BL/6J mice (control) and mice with liver-specific deletion of STARD1 (*Stard1*$^{\Delta Hep}$), SAB (*Sab*$^{\Delta Hep}$), or JNK1 and JNK2 (*Jnk1*+2$^{\Delta Hep}$) were given VPA with or without APAP. Liver tissues were collected and analyzed by histology and immunohistochemistry and for APAP metabolism, endoplasmic reticulum (ER) stress, and mitochondrial function. Adult human hepatocytes were transplanted into Fah$^{-/-}$/Rag2$^{-/-}$/Il2rg$^{-/-}$/NOD (FRGN) mice to create mice with humanized livers. **RESULTS:** Administration of VPA before administration of APAP increased the severity of liver damage in control mice. The combination of VPA and APAP increased expression of CYP2E1, formation of NAPQI-protein adducts, and depletion of glutathione from liver tissues of control mice, resulting in ER stress and the upregulation of STARD1. Livers from control mice given VPA and APAP accumulated cholesterol in the mitochondria and had sustained mitochondrial depletion of glutathione and mitochondrial dysfunction. Inhibition of ER stress, by administration of tauroursodeoxycholic acid to control mice, prevented upregulation of STARD1 in liver and protected the mice from hepatoxicity following administration of VPA and APAP. Administration of N-acetylcysteine to control mice prevented VPA- and APAP-induced ER stress and liver injury. *Stard1*$^{\Delta Hep}$ mice were resistant to induction of ALF by VPA and APAP, despite increased mitochondrial levels of glutathione and phosphorylated JNK; we made similar observations in fasted *Stard1*$^{\Delta Hep}$ mice given APAP alone. *Sab*$^{\Delta Hep}$ mice or *Jnk1*+2$^{\Delta Hep}$ mice did not develop ALF following administration of VPA and APAP. The ability of VPA to increase the severity of APAP-induced liver damage was observed in FRGN mice with humanized liver. **CONCLUSIONS:** In studies of mice, we found that upregulation of STARD1 following ER stress mediates APAP hepatoxicity via SH3BP5 and phosphorylation of JNK1 and JNK2.

Keywords: Mouse Model; Signal Transduction; Lipid; APAP Toxicity.

Drug-induced liver injury (DILI) is a major cause of acute liver failure (ALF) and a leading reason for drug withdrawal from the market.[1,2] Unlike intrinsic DILI, which is predictable, reproducible, and dose-dependent, idiosyncratic DILI is unpredictable, not strictly dose-dependent, and although rare it accounts for 10% to 15% of ALF cases in the United States.[3,4]

Acetaminophen (APAP) is one of the most widely used pain relievers worldwide. Although relatively safe, APAP is a dose-dependent hepatotoxin that can cause intrinsic DILI. The use of APAP at therapeutic doses for more than a few days has been shown to elevate serum transaminases in one-third of patients.[5] Acetaminophen-induced liver damage is characterized by hemorrhagic centrilobular necrosis and high plasma transaminase levels in both humans and animals, which can evolve in some cases to ALF.[6] Although APAP is metabolized to its glucuronidated and sulphated nontoxic metabolites in the liver, APAP overdose saturates these pathways and the excess APAP is metabolized by CYP2E1 into the reactive metabolite N-acetyl-p-benzoquinoneimine (NAPQI), which is rapidly conjugated with glutathione, resulting in nontoxic mercapturic acid and cysteine conjugates that are excreted in the urine.[7,8] When glutathione levels are limited, free unconjugated NAPQI reacts with sulfhydryl groups on cysteine and lysine residues, generating NAPQI-protein adducts (APAP-protein adducts) in hepatocytes, particularly in mitochondria, leading to mitochondrial dysfunction and cell death.[7–9] SH3BP5 (Sab), a mitochondrial outer membrane protein, has been identified as a key player in APAP-induced hepatotoxicity. Knockdown or liver-specific knockout of SH3BP5 inhibited sustained c-Jun N-terminal kinase (JNK) activation and protected against APAP hepatotoxicity.[10] Moreover, there is extensive experimental evidence that JNK activation and its translocation to mitochondria contribute to APAP hepatotoxicity.[11,12]

Valproic acid (VPA) is widely prescribed for epilepsy and used as an anticonvulsant, which is eliminated by biotransformation through multiple pathways, including glucuronidation, cytochrome P-450 metabolism, and mitochondrial β-oxidation.[13] Besides inducing metabolic syndrome in overweight epileptic patients,[14,15] long-term VPA therapy can cause hepatotoxicity that may progress to idiosyncratic ALF.[13,16] VPA-mediated hepatotoxicity is characterized by necrosis, depletion of endogenous antioxidants, and disruption of mitochondrial β-oxidation of fatty acids, which can contribute to hepatic steatosis.[16–20] Furthermore, VPA has been shown to inhibit HDAC and GSK3 signaling events,[21,22] and although reported to induce endoplasmic reticulum stress (ER stress),[23,24] there are studies showing that VPA protects cells against ER stress–mediated apoptosis and atherosclerosis.[25,26]

As VPA has been shown to deplete glutathione levels and stimulate steroidogenesis by increasing mitochondrial cholesterol trafficking,[27,28] we hypothesized that VPA can sensitize to APAP-mediated ALF independently of fasting by inducing steroidogenic acute regulatory protein 1 (STARD1), a mitochondrial protein that mediates the transport of cholesterol to the mitochondrial inner membrane,[29] which results in impaired transport of glutathione into mitochondria.[30,31] Our data reveal that VPA pretreatment in nonfasted mice results in APAP-induced ALF by a mechanism that requires the complimentary action of STARD1 and Sab-JNK1/2.

WHAT YOU NEED TO KNOW

BACKGROUND AND CONTEXT

Acetaminophen overdose is a major cause of acute liver failure. Mitochondrial SH3BP5 and phosphorylation of JNK mediate the hepatotoxic effects of acetaminophen.

NEW FINDINGS

Administration of valproic acid (VPA) to mice was found to increase the severity of acetaminophen-induced liver damage, via increased expression of steroidogenic acute regulatory protein (STARD1), and SH3BP5 and phosphorylation of JNK1 and JNK2.

LIMITATIONS

This study was performed in mice.

IMPACT

Strategies to block the STARD1 signaling pathway might be developed to treat acetaminophen-induced liver injury.

Materials and Methods

Generation of Mice With Liver-Specific STARD1 Deletion

All experimental protocols for animal use and handling met the guidelines of the Animal Care Committee of the Hospital Clinic-Universidad de Barcelona. Male C57BL/6J mice (8 weeks of age) were obtained from Charles River Laboratories (Wilmington, MA). As mice with global STARD1 deletion die soon after birth due to adrenal lipoid hyperplasia,[32] we generated mice with liver-specific STARD1 deletion by Cre-lox technology, as described in Supplementary Methods (Supplementary Figure 1*A*). Homozygous Stard1 floxed animals ($STARD1^{f/f}$) were crossed with albumin-Cre mice (C57BL/6-TgN[Alb-Cre]^{21Mgn}; Jackson Laboratories) to obtain $Stard1^{f/f\text{-}AlbCre}$ (Stard1 Liver-specific knockout, $STARD1^{\Delta Hep}$), which exhibited

* Authors share co-first authorship; § Authors share co-senior authorship.

Abbreviations used in this paper: **ALF, acute liver failure; APAP, acetaminophen; DILI, drug-induced liver injury; ER stress, endoplasmic reticulum stress; FAH, fumarylacetoacetate hydrolase; FRGN, $Fah^{-/-}$/$Rag2^{-/-}$/$Il2rg^{-/-}$/NOD; H&E, hematoxylin-eosin; HH, human adult hepatocytes; JNK, c-Jun N-terminal kinase; mRNA, messenger RNA; NAC, N-acetylcysteine; NAPQI, N-acetyl-p-benzoquinoneimine; PMH, primary mouse hepatocyte; STARD1, steroidogenic acute regulatory protein 1; TUDCA, tauroursodeoxycholic acid; TUNEL, terminal deoxynucleotidyl transferase–mediated deoxyuridine triphosphate nick-end labeling; VPA, valproic acid.**

Most current article

0016-5085
https://doi.org/10.1053/j.gastro.2019.04.023

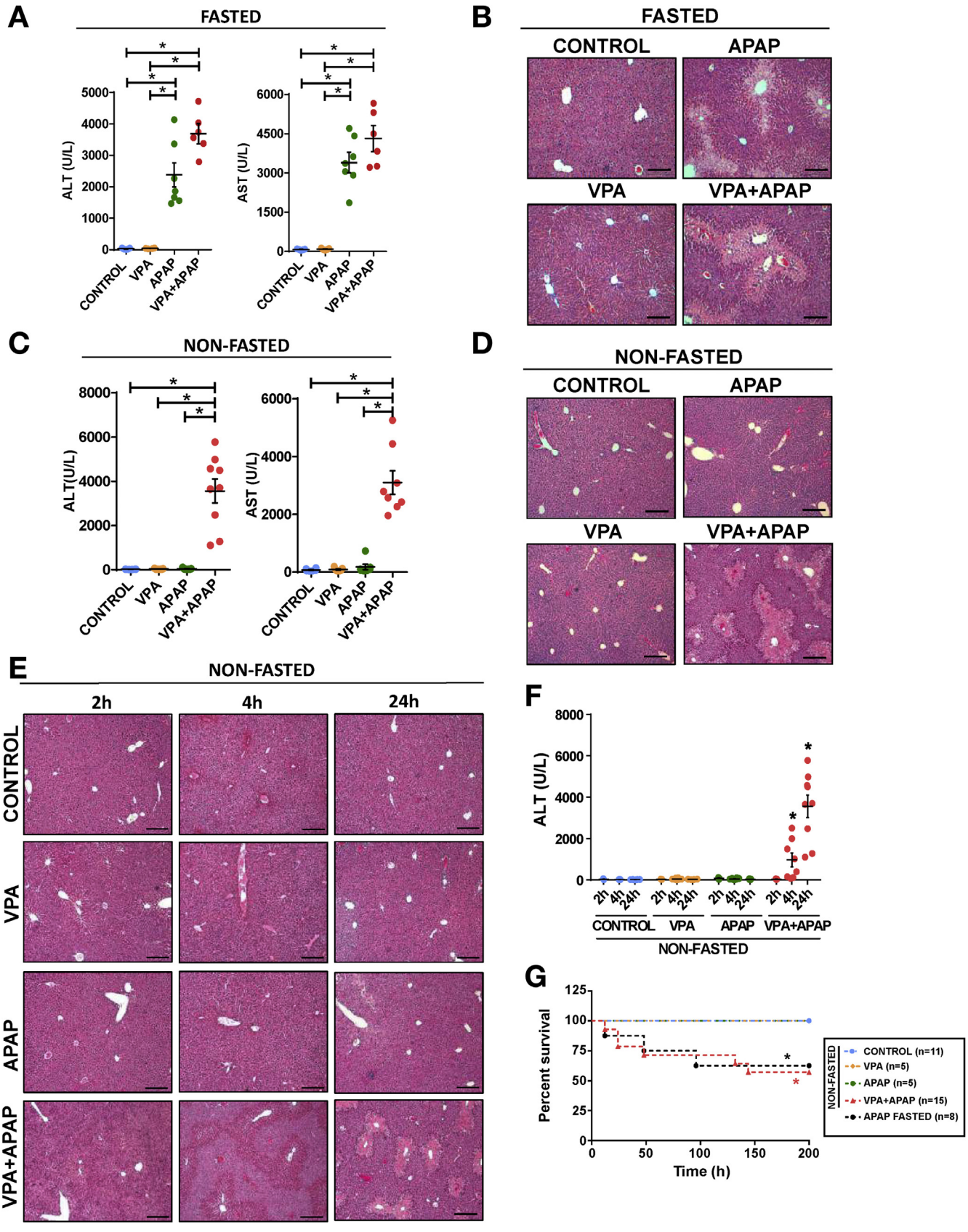
A
FASTED
ALT (U/L)
AST (U/L)
CONTROL
VPA
APAP
VPA+APAP
B
FASTED
CONTROL
APAP
VPA
VPA+APAP
C
NON-FASTED
ALT(U/L)
AST (U/L)
D
NON-FASTED
E
NON-FASTED
2h
4h
24h
F
ALT (U/L)
NON-FASTED
G
Percent survival
Time (h)
NON-FASTED
CONTROL (n=11)
VPA (n=5)
APAP (n=5)
VPA+APAP (n=15)
APAP FASTED (n=8)

specific deletion of Stard1 in the liver with unchanged expression in steroidogenic tissues and white adipose tissue (Supplementary Figure 1*B* and *C*). Mice were backcrossed to C57BL/6J strain for 9 generations. Eight- to 10-week-old STARD1$^{f/f}$ littermates and STARD1$^{\Delta Hep}$ mice were treated with VPA, APAP, and their combination as described as follows.

Mice With Liver-Specific Deletion of Sab and JNK1+2

Sab$^{\Delta Hep}$ (C57BL/6N) and JNK1+2$^{\Delta Hep}$ (57BL/6J) mice were generated by treatment of Sab$^{f/f}$ mice or JNK1+2$^{f/f}$ with AAV8.TBG.Cre as described previously.[10] JNK1+2$^{f/f}$ mice were provided by Dr Roger J. Davis (UMass Medical School, Worcester, MA).

FRGN Mice With Humanized Liver and Expansion of Human Hepatocytes

Fah$^{-/-}$/Rag2$^{-/-}$/Il2rg$^{-/-}$/NOD (FRGN) mice were xenotransplanted with human adult hepatocytes (HHs), as described before,[33] achieving a rate of repopulation of 80% to 90% as monitored by serum human albumin levels. Experiments to determine susceptibility to VPA and APAP were conducted in 14-week-old FRGN mice in accordance with the approved Institutional Animal Care Committee at Oregon Health & Science University of Portland, Oregon, and Animal Care Committee of the Hospital Clinic-Universidad de Barcelona. Plateable cryopreserved male HHs (#M00995-P) were obtained from BioreclamationIVT Company (Brussels, Belgium). One million viable HHs in 100 μL Dulbecco's modified essential medium were injected intrasplenically via a 27-gauge needle followed by gradual reduction of 2-(2-nitro-4-trifluoromethylbenzoyl)-1,3-cyclohexanedione 1 week after xenotransplantation, as described.[33]

In Vivo Treatment With VPA and APAP

Eight- to 10-week-old C57BL/6J, STARD1$^{\Delta Hep}$, Sab$^{\Delta Hep}$, and JNK1+2$^{\Delta Hep}$ mice were treated with VPA, 400 mg/kg subcutaneously, a dosage typically used in mice,[34,35] 3 times every 12 hours followed by a single APAP injection (300 mg/kg intraperitoneally [IP]). Determination of serum VPA levels (Dimension EXL analyzer; Siemens Healthcare, Erlangen, Germany) from mice treated with 400 mg/kg were 38.0 ± 2.4 μg/mL, similar to the therapeutic range reported in patients under VPA therapy.[36] Mice were killed at 2, 4, or 24 hours after receiving APAP and serum and liver samples were collected for analyses. In addition, APAP hepatotoxicity was induced in overnight fasted mice. In some cases, tauroursodeoxycholic acid (TUDCA; 250 mg/kg IP; Calbiochem, San Diego, CA) or N-acetylcysteine (NAC; 2.5 mmol/kg IP) were administered 3 times every 12 hours along with VPA and APAP treatment. Other groups of mice were dosed with atorvastatin (10 mg/kg, daily) or vehicle via gavage along with VPA followed by APAP administration.

Statistical Analyses

Results are expressed as mean ± standard error of the mean. Statistical significance of mean values were assessed using Student *t*-test (2 groups) and 1- or 2-way analysis of variance followed by Tukey's Multiple Comparison Post-test (≥ 3 groups). $P < .05$ was considered statistically significant. Survival curves were constructed using the method of Kaplan and Meier. The corresponding number of experiments are indicated in the figure legends. Statistics were performed using GraphPad Prism 6 software (La Jolla, CA).

Results

Fasting or VPA Pretreatment in Nonfasted Mice Sensitizes to APAP Hepatotoxicity

As fasting sensitizes to APAP-mediated hepatotoxicity,[37] we first examined whether fasting potentiated the hepatotoxicity of VPA+APAP coadministration. Although repeated VPA dosing to fasted mice did not cause hepatotoxicity, APAP administration induced marked liver injury and centrilobular necrosis (Figure 1*A* and *B*); however, the combination of VPA+APAP did not further enhance the liver injury caused by APAP alone, indicating that fasting sensitized to APAP hepatotoxicity regardless of VPA pretreatment. In contrast, nonfasted mice were resistant to APAP-induced liver injury when APAP was given in the morning, in agreement with previous results,[38] and VPA administration (3 times/12 hours) did not cause liver damage (Figure 1*C* and *D*). Interestingly, VPA preadministration in nonfasted mice sensitized to APAP-mediated hepatotoxicity similar to the injury seen in fasted mice following APAP administration (Figure 1*C* and *D*), with increased alanine aminotransferase (ALT) release over time, which paralleled the liver injury seen by hematoxylin-eosin (H&E) (Figure 1*E* and *F*). We next examined the survival of nonfasted mice to VPA pretreatment followed by the administration of a higher dose of APAP (600 mg/kg). Although nonfasted mice were resistant to VPA or APAP alone, mice pretreated with VPA followed by APAP administration died over time with a mortality rate of 40% by 8 days post-APAP administration that was similar to the rate observed in fasted mice after being given APAP (Figure 1*G*). Moreover, treatment with VPA+APAP caused a higher rate of cell death in primary mouse hepatocytes (PMHs) as

Figure 1. VPA pretreatment sensitizes to APAP hepatotoxicity in nonfasted mice. (*A*, *B*) Fasted mice were given VPA (400 mg/kg 3 times/12 hours; n = 5 mice), APAP (300 mg/kg, n = 7 mice), or VPA+APAP (n = 6 mice) and killed 24 hours later to examine ALT/aspartate aminotransferase (AST) and H&E analysis. (*C*, *D*) Nonfasted mice were killed 24 hours after VPA (400 mg/kg 3 times/12 hours; n = 5 mice), APAP (300 mg/kg; n = 6 mice) or VPA+APAP (n = 9 mice) to determine ALT/AST and H&E. (*E*, *F*) Nonfasted mice were killed at 2, 4, and 24 hours after VPA, APAP, or VPA+APAP to examine H&E and ALT levels. (*G*) Time-dependent survival of nonfasted mice given VPA (400 mg/kg 3 times/12 hours), APAP (600 mg/kg), or VPA+APAP. For comparison, survival rate was determined in mice treated with a single injection of APAP (600 mg/kg) after overnight fasting. Scale bars: 100 μm. The number of mice in (*G*) is shown in the graph. *$P < .05$ as indicated.

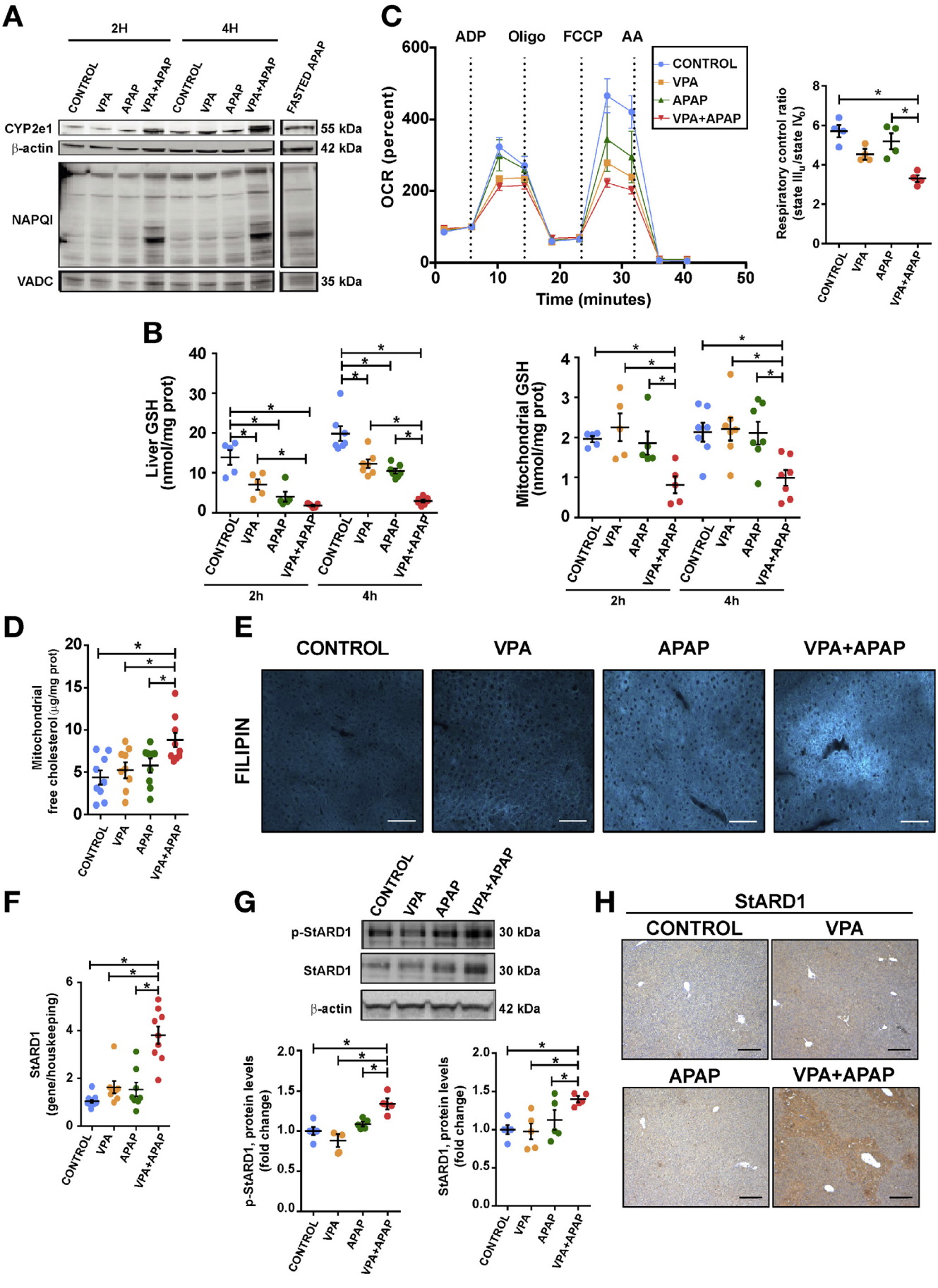
A
2H
4H
CONTROL
VPA
APAP
VPA+APAP
FASTED APAP
CYP2e1
β-actin
NAPQI
VADC
55 kDa
42 kDa
35 kDa
C
ADP
Oligo
FCCP
AA
OCR (percent)
Time (minutes)
Respiratory control ratio (state IIIu/state IVo)
B
Liver GSH (nmol/mg prot)
Mitochondrial GSH (nmol/mg prot)
2h
4h
D
Mitochondrial free cholesterol (μg/mg prot)
E
FILIPIN
F
StARD1 (gene/housekeeping)
G
p-StARD1
StARD1
30 kDa
p-StARD1, protein levels (fold change)
StARD1, protein levels (fold change)
H
StARD1

revealed by Sytox Green staining compared with either drug alone (Supplementary Figure 2*A*).

APAP Metabolism, Glutathione Homeostasis, and Mitochondrial Function Following VPA+APAP Administration in Nonfasted Mice

Unlike VPA or APAP alone, VPA+APAP coadministration to nonfasted mice induced an early and time-dependent upregulation of CYP2E1 that paralleled the generation of NAPQI-protein adducts, similar to the levels induced by APAP in fasted mice (Figure 2*A*). Moreover, as glutathione is required for NAPQI detoxification, we next examined glutathione homeostasis in liver homogenate and mitochondrial fraction in nonfasted mice. As seen, total glutathione levels were moderately depleted 2 hours after VPA or APAP alone, which increased by 4 hours posttreatment and recovered to control levels by 24 hours, whereas total glutathione levels remained significantly depleted at 4 hours after VPA+APAP administration (Figure 2*B*), consistent with the kinetics of NAPQI-protein adduct formation. However, neither VPA nor APAP alone affected mitochondrial glutathione levels, whereas the combination of VPA+APAP markedly depleted mitochondrial glutathione stores as early as 2 hours posttreatment that remained significantly decreased by 4 hours (Figure 2*B*). In line with the induction of CYP2E1 or NAPQI-adduct generation, APAP administration to fasted mice depleted total and mitochondrial glutathione levels by 65% to 75%, similar to the depletion induced by VPA+APAP administration in fed mice.

We next examined mitochondrial function using a metabolic flux analyzer to determine real-time oxygen consumption rates. Although VPA or APAP alone did not affect mitochondrial function, VPA+APAP coadministration resulted in a decreased respiratory control ratio (State III/State IV) with respect to VPA or APAP alone (Figure 2*C*), indicating impaired mitochondrial respiration.

VPA+APAP Upregulates STARD1 Expression in Nonfasted Mice

We next examined the homeostasis of cholesterol and its trafficking to mitochondria, which is known to regulate mitochondrial glutathione.[30,31] Interestingly, increased mitochondrial pool of cholesterol was an early event (4 hours) after giving VPA+APAP (Figure 2*D*), even though free cholesterol levels increased afterward, as shown by the representative filipin staining at 24 hours (Figure 2*E*), suggesting the activation of a specific mechanism that triggers the accumulation of free cholesterol in mitochondria. As STARD1 regulates mitochondrial cholesterol trafficking,[29] we next examined its expression in response to drug administration. In contrast to VPA or APAP alone, VPA+APAP increased an early expression (4 hours) of STARD1 both at the messenger RNA (mRNA) and protein levels (Figure 2*F* and *G*). To examine the pattern of STARD1 expression, we performed immunohistochemical analysis in liver sections 24 hours after VPA+APAP administration (Figure 2*H*), indicating predominant expression in the pericentral area, which is consistent with the characteristic hemorrhagic centrilobular necrosis seen in APAP hepatotoxicity. These findings were accompanied by increased expression of phosphorylated STARD1 (Figure 2*G*), which is known to increase its activity in the trafficking of cholesterol to mitochondria in steroidogenic cells.[39,40] Moreover, the expression of hepatic MLN64 (also known as STARD3), another member of the STARD family involved in the egress of cholesterol from endosomes to mitochondria,[41,42] did not significantly increase at early time points after VPA+APAP administration (Supplementary Figure 3*A*), although it increased 24 hours posttreatment.

VPA+APAP Induces ER Stress and Mitochondrial JNK Activation in Nonfasted Mice

As tunicamycin has been shown to induce the expression of STARD1 by triggering ER stress rather than SREBP2 activation,[43] and consistent with the role of ER stress in the regulation of STAR family members,[44,45] we next examined ER stress as a potential mechanism that regulates STARD1 expression. VPA+APAP induced an early (2 hours) increase in the expression of several ER stress markers at the mRNA and protein levels (Figure 3*A* and *B*). The increase of ER stress markers was sustained at 4 hours posttreatment (Figure 3*C* and *D*), suggesting the involvement of different arms of the ER stress pathway (eg, IRE-1α and PERK). Moreover, immunohistochemical analyses revealed that VPA+APAP increased CHOP expression in liver sections 24 hours posttreatment (Figure 3*E*), which exhibited predominant pericentral staining, similar to STARD1. Because

Figure 2. Mitochondrial dysfunction and STARD1 upregulation by VPA+APAP. (*A*, *B*) Nonfasted mice were given VPA (400 mg/kg 3 times/12 hours; n $\geq$ 5 mice), APAP (300 ng/kg; n $\geq$ 5 mice) or VPA+APAP (n $\geq$ 5 mice) and killed 2 and 4 hours posttreatment for CYP2E1 levels and NAPQI-protein adducts generation or glutathione (GSH) levels in total liver extracts or mitochondrial fraction. As positive control, CYP2E1 and NAPQI-adducts were determined in fasted mice after 2 hours of APAP administration. (*C*) Oxygen consumption rate tracings and respiratory control ratio of isolated mitochondria from nonfasted mice treated with VPA (n = 4 mice), APAP (n = 4 mice), or VPA+APAP (n = 4 mice) for 4 hours. (*D*) Mitochondrial cholesterol levels of nonfasted mice 4 hours after treatment with VPA (n = 9 mice), APAP (n = 9 mice), or VPA+APAP (n = 9 mice). (*E*) Filipin staining of frozen liver sections from nonfasted mice 24 hours after treatment with VPA, APAP, or VPA+APAP. Scale bar: 50 μm. (*F*) STARD1 mRNA levels from liver extracts of nonfasted mice 4 hours after treatment with VPA (n = 8 mice), APAP (n = 8 mice), or VPA+APAP (n = 9 mice). (*G*) STARD1 and p-STARD1 expression in liver extracts of nonfasted mice 4 hours after treatment with VPA (n = 5 mice), APAP (n = 5 mice), or VPA+APAP (n = 5 mice). (*H*) Immunohistochemical staining of STARD1 in liver sections from nonfasted mice 24 hours after treatment with VPA, APAP, or VPA+APAP. Scale bar: 100 μm. *$P < 0.05$ as indicated.

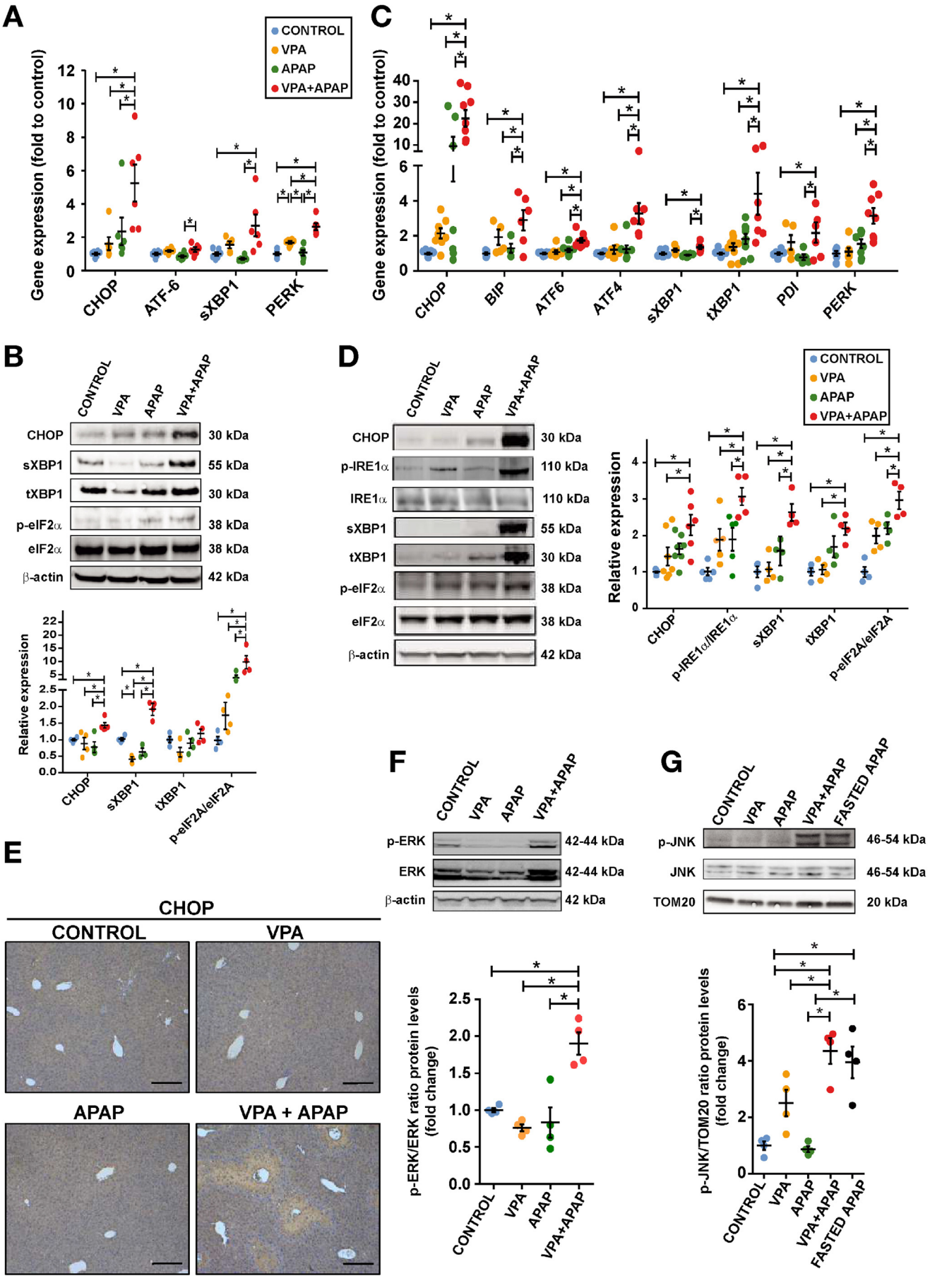
A
CONTROL
VPA
APAP
VPA+APAP
Gene expression (fold to control)
CHOP
ATF-6
sXBP1
PERK
C
Gene expression (fold to control)
CHOP
BIP
ATF6
ATF4
sXBP1
tXBP1
PDI
PERK
B
CONTROL
VPA
APAP
VPA+APAP
CHOP 30 kDa
sXBP1 55 kDa
tXBP1 30 kDa
p-eIF2α 38 kDa
eIF2α 38 kDa
β-actin 42 kDa
Relative expression
CHOP
sXBP1
tXBP1
p-eIF2A/eIF2A
D
CONTROL
VPA
APAP
VPA+APAP
CHOP 30 kDa
p-IRE1α 110 kDa
IRE1α 110 kDa
sXBP1 55 kDa
tXBP1 30 kDa
p-eIF2α 38 kDa
eIF2α 38 kDa
β-actin 42 kDa
Relative expression
CHOP
p-IRE1α/IRE1α
sXBP1
tXBP1
p-eIF2A/eIF2A
E
CHOP
CONTROL
VPA
APAP
VPA + APAP
F
CONTROL
VPA
APAP
VPA+APAP
p-ERK 42-44 kDa
ERK 42-44 kDa
β-actin 42 kDa
p-ERK/ERK ratio protein levels (fold change)
CONTROL
VPA
APAP
VPA+APAP
G
CONTROL
VPA
APAP
VPA+APAP
FASTED APAP
p-JNK 46-54 kDa
JNK 46-54 kDa
TOM20 20 kDa
p-JNK/TOM20 ratio protein levels (fold change)
CONTROL
VPA
APAP
VPA+APAP
FASTED APAP

ERK1/2 phosphorylates and regulates STARD1 activity,[46] we next analyzed the expression of hepatic ERK1/2 in mice treated with VPA+APAP. As seen, the phospho-ERK/ERK increased 4 hours after VPA+APAP compared with either drug alone (Figure 3*F*). In addition, we also examined whether VPA+APAP enhanced the translocation of phosphorylated JNK to mitochondria, which has emerged as a crucial event for acute liver injury.[10,11] As seen, increased translocation of phosphorylated JNK in mitochondria was observed 2 hours after VPA+APAP, similar to the increase seen by APAP treatment in fasted mice (Figure 3*G*).

Targeting ER Stress Prevents STARD1 Upregulation and Protects Against VPA+APAP Hepatotoxicity in Nonfasted Mice

We examined the impact of interfering with ER stress on STARD1 expression and liver injury by VPA+APAP administration. As seen, TUDCA abolished the induction of ER stress markers CHOP, sXBP1, and p-EIF2α 4 hours post-treatment with VPA+APAP (Figure 4*A*). In line with these findings, TUDCA prevented the increased expression of CHOP in liver sections (24 hours) after VPA+APAP (Figure 4*B*). Consistent with the induction of STARD1 by tunicamycin-induced ER stress,[44] TUDCA prevented the early (4 hours) STARD1 upregulation by VPA+APAP (Figure 4*C* and *D*) and the sustained expression of STARD1 in liver sections as revealed by immunohistochemistry (24 hours) (Figure 4*E*) and its mitochondrial targeting examined by confocal imaging (Supplementary Figure 4). More importantly and in line with these events, TUDCA prevented the mitochondrial glutathione depletion induced by VPA+APAP (Figure 4*F*) and protected against liver injury caused by VPA+APAP administration (Figure 4*G* and *H*).

Arylating quinones have been shown to induce ER stress,[47] and correct protein folding in the ER requires appropriate redox environment. Thus, we addressed whether in addition to the role of NAPQI glutathione depletion can contribute to ER stress. PMH treated with diethylmaleate severely depleted total glutathione content and increased the level of CHOP, indicating the onset of ER stress (Supplementary Figure 2*B* and *C*). In addition, diethylmaleate-induced CHOP upregulation was attenuated by glutathione replenishment with NAC (Supplementary Figure 2*C*). Moreover, tunicamycin induced CHOP expression, as expected, that was ameliorated by NAC, suggesting a relationship between glutathione and ER stress regulation. Furthermore, in line with these in vitro findings, in vivo NAC administration to mice given VPA+APAP restored total glutathione and mitochondrial glutathione stores (Figure 5*A*) and, importantly, prevented VPA+APAP-induced ER stress (Figure 5*B* and *C*) and subsequent STARD1 induction (Figure 5*D* and *E*), resulting in the protection against VPA+APAP-mediated liver injury (Figure 5*F* and *G*).

Liver-Specific STARD1 Deletion Protects Against APAP Hepatotoxicity Elicited by VPA or Fasting

STARD1$^{\Delta Hep}$ mice were generated by crossing chimeric STARD1$^{f/f}$ mice with Alb-Cre mice (Supplementary Figure 1*A*–*C*). STARD1$^{\Delta Hep}$ mice exhibited a marked down-regulation of STARD1 expression in liver extracts which did not affect the mitochondrial number and morphology (Supplementary Figure 1*D*). As seen, VPA+APAP induced the expression of STARD1 in STARD1$^{f/f}$ mice at the mRNA and protein levels in liver homogenates and liver samples as revealed by immunohistochemistry, which were abolished in STARD1$^{\Delta Hep}$ mice (Figure 6*A*–*C*). This outcome was specific for STARD1 as expression of MLN64 by VPA+APAP was maintained in STARD1$^{\Delta Hep}$ mice (Supplementary Figure 3*B*). As expected, VPA+APAP increased mitochondrial cholesterol levels in STARD1$^{f/f}$ but not STARD1$^{\Delta Hep}$ mice (Figure 6*D*), which translated in higher levels of mitochondrial glutathione in STARD1$^{\Delta Hep}$ mice by VPA+APAP administration (Figure 6*E*). Consistent with these findings, VPA+APAP-induced liver injury examined by serum ALT levels and H&E was markedly lower in STARD1$^{\Delta Hep}$ mice with respect to STARD1$^{f/f}$ mice (Figure 6*F* and *G*, Supplementary Figure 5). Moreover, adenovirus-mediated STARD1 knockdown also prevented VPA+APAP-mediated hepatotoxicity in nonfasted mice (Supplementary Figure 6), further validating the relevance of STARD1 activation in the hepatotoxic effects caused by VPA+APAP administration. In addition, similar protection was observed following APAP administration in overnight fasted STARD1$^{\Delta Hep}$ mice, without preventing the induction of CYP2E1 and ER stress (Figure 7). Moreover, as a complementary approach to test the role of cholesterol in VPA+APAP-induced liver injury, atorvastatin prevented the increase in mitochondrial cholesterol levels and protected against VPA+APAP-mediated liver injury (Supplementary Figure 7).

We examined whether the protection of STARD1$^{\Delta Hep}$ mice was related to a lower translocation of phosphorylated

Figure 3. VPA+APAP induces ER stress in nonfasted mice. (*A*) mRNA levels of ER stress markers in liver extracts of nonfasted mice 2 hours after treatment with VPA (400 mg/kg; 3 times/12 hours; n $\geq$ 5 mice), APAP (300 mg/kg; n $\geq$ 5 mice) or VPA+APAP (n $\geq$ 5 mice). (*B*) Western blots of ER stress markers in liver extracts of nonfasted mice 2 hours after treatment with VPA (400 mg/kg; 3 times/12 hours; n = 4 mice), APAP (300 mg/kg; n = 4 mice), or VPA+APAP (n = 4 mice). (*C*) mRNA levels of ER stress markers 4 hours after treatment with VPA (n $\geq$ 5 mice), APAP (n $\geq$ 5 mice), or VPA+APAP (n $\geq$ 5 mice). (*D*) Western blots of ER stress markers in liver extracts of nonfasted mice 4 hours after treatment with VPA (n $\geq$ 4 mice), APAP (n $\geq$ 4 mice), or VPA+APAP (n $\geq$ 4 mice). (*E*) Immunohistochemistry of CHOP expression in livers of nonfasted mice 24 hours after treatment with VPA, APAP, or VPA+APAP. Scale bar: 100 μm. (*F*) Phospho-ERK activation in liver extracts from nonfasted mice 4 hours after treatment with VPA (n = 4 mice), APAP (n = 4 mice), or VPA+APAP (n = 4 mice). (*G*) Phospho-JNK levels in mitochondrial fractions from nonfasted mice treated for 2 hours with VPA (n = 4 mice), APAP (n = 4 mice), or VPA+APAP (n = 4 mice). *$P < .05$ as indicated.

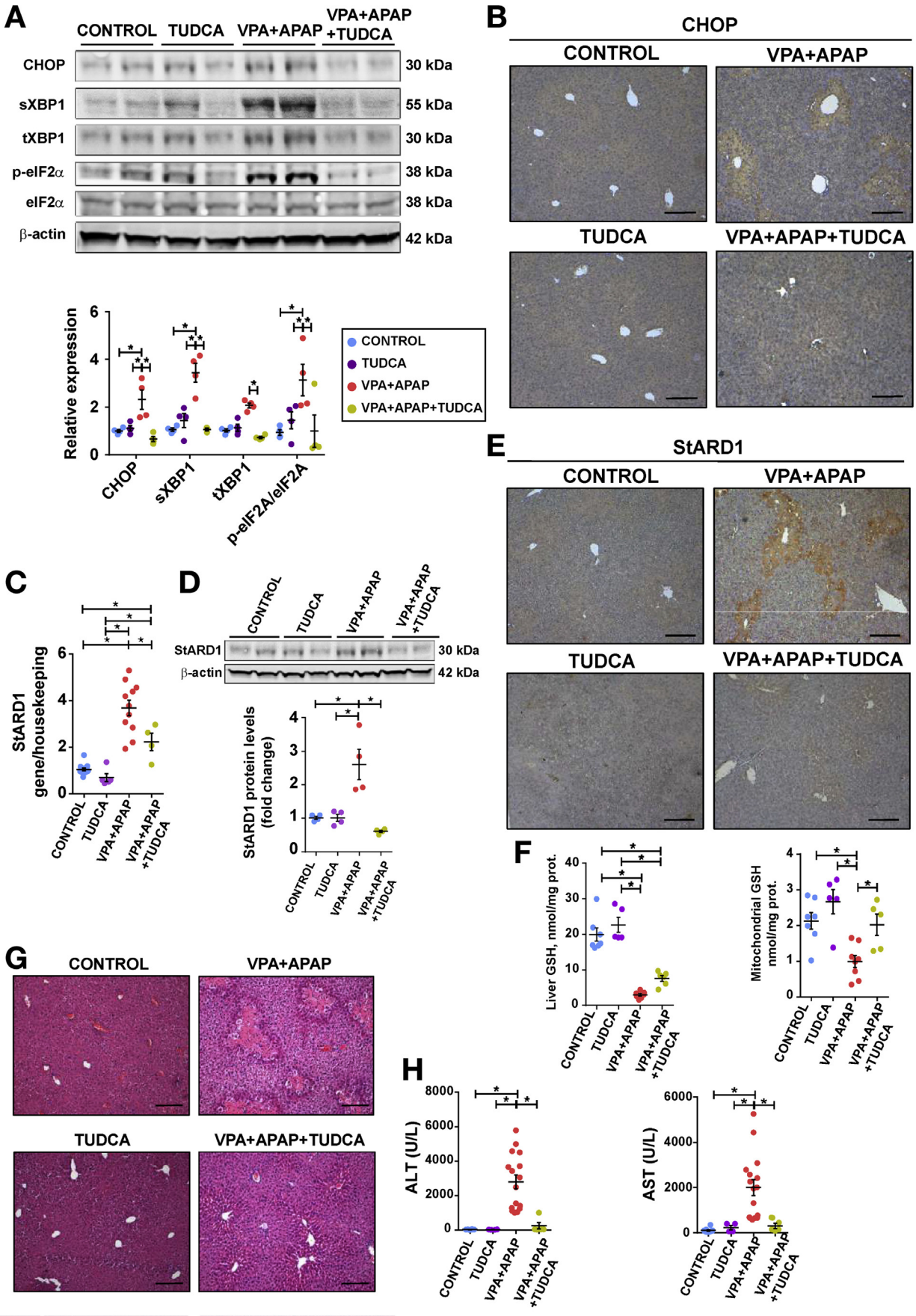
A
CONTROL
TUDCA
VPA+APAP
VPA+APAP +TUDCA
CHOP
sXBP1
tXBP1
p-eIF2α
eIF2α
β-actin
30 kDa
55 kDa
30 kDa
38 kDa
38 kDa
42 kDa
Relative expression
CONTROL
TUDCA
VPA+APAP
VPA+APAP+TUDCA
CHOP
sXBP1
tXBP1
p-eIF2A/eIF2A
B
CHOP
CONTROL
VPA+APAP
TUDCA
VPA+APAP+TUDCA
E
StARD1
CONTROL
VPA+APAP
TUDCA
VPA+APAP+TUDCA
C
StARD1 gene/housekeeping
D
StARD1
β-actin
30 kDa
42 kDa
StARD1 protein levels (fold change)
F
Liver GSH, nmol/mg prot.
Mitochondrial GSH nmol/mg prot.
G
CONTROL
VPA+APAP
TUDCA
VPA+APAP+TUDCA
H
ALT (U/L)
AST (U/L)

JNK to mitochondria. As seen, the mitochondrial phosphorylation of JNK induced by VPA+APAP was similar in both STARD1$^{f/f}$ and STARD1$^{\Delta Hep}$ mice (Figure 6*H*), with similar findings observed in overnight fasted STARD1$^{f/f}$ and STARD1$^{\Delta Hep}$ mice following APAP administration (Figure 7*E*). These results indicate that mitochondrial translocation of phosphorylated JNK requires STARD1 to elicit liver injury.

Mice With Liver-Specific Deletion of Sab and JNK1+2 Are Protected Against VPA+APAP-Induced Liver Injury

We next examined the role of Sab and JNK in the liver injury in nonfasted mice given VPA+APAP. Nonfasted Sab$^{\Delta Hep}$ mice and JNK1+2$^{\Delta Hep}$ mice were administered with repeated doses of VPA followed by a single APAP administration. Although both Sab$^{f/f}$ mice and JNK1+2$^{f/f}$ mice were sensitized to APAP-induced liver injury by VPA pretreatment as shown by H&E analyses and serum ALT release, Sab$^{\Delta Hep}$ mice and JNK1+2$^{\Delta Hep}$ mice were markedly protected against VPA+APAP-induced liver damage (Supplementary Figure 8*A–D*). Quite interestingly, although VPA+APAP induced STARD1 and CHOP in Sab$^{f/f}$ mice and JNK1+2$^{f/f}$ mice, these effects were prevented in Sab$^{\Delta Hep}$ and JNK1+2$^{\Delta Hep}$ mice, suggesting that Sab/JNK is necessary for ER stress and subsequent STARD1 induction (Supplementary Figure 8*E* and *F*). Similar results were observed in fasted JNK1+2$^{\Delta Hep}$ mice after APAP administration (Figure 7*F*). These findings together with the protection seen in STARD1$^{\Delta Hep}$ mice suggest that STARD1 and Sab-JNK1+2 exert complementary roles in APAP-induced liver injury.

VPA Sensitizes to APAP Hepatotoxicity in FRGN Mice With Humanized Liver

To address the potential translational relevance of the preceding findings showing the sensitization of VPA to APAP-mediated hepatotoxicity, we next explored the susceptibility of FRGN mice, a genetically engineered model that allows the repopulation of the murine liver with HH, to VPA+APAP-induced liver injury. FRGN mice were repopulated with HHs by more than 80% as revealed by the human albumin levels in serum and the expression of human fumarylacetoacetate hydrolase (FAH) (Supplementary Figure 9*A* and *B*). Nonfasted FRGN mice were treated with VPA followed by a single dose of APAP and killed 24 hours after treatment. Although nonfasted FGRN mice xenotransplanted with HHs were resistant to VPA or APAP, their combination caused liver injury, as revealed by increased serum transaminases and H&E analyses (Supplementary Figure 9*C* and *D*). In line with these findings, humanized FRGN mice given VPA+APAP exhibited depletion of both total glutathione and mitochondrial glutathione levels (Supplementary Figure 10*A*), as well as an increase in the expression of ER stress markers (Supplementary Figure 10*B*), and an early increase in STARD1 mRNA levels (Supplementary Figure 10*C*), in parallel with the increased STARD1 expression in liver sections (Supplementary Figure 9*E*) and enhanced MLN64 expression (Supplementary Figure 3*D*). Moreover, although endogenous staining of F4/80 and myeloperoxidase in humanized FRGN mice was low,[48] VPA+APAP induced a mild expression of F4/80 with a minimal staining of myeloperoxidase (Supplementary Figure 10*D*). To validate whether this outcome reflected the injury of HHs rather than the remnant murine hepatocytes by VPA+APAP, we estimated the colocalization of FAH expression with terminal deoxynucleotidyl transferase–mediated deoxyuridine triphosphate nick-end labeling (TUNEL) as a measure of damaged HHs. As seen, most TUNEL-positive cells colocalized with HHs expressing FAH (Supplementary Figure 9*F* and *G*). Thus, these findings underscore the susceptibility of in vivo repopulation of HHs to VPA+APAP hepatotoxicity.

Discussion

Here, we uncover that although nonfasted mice are resistant to VPA or APAP administration, prior VPA dosing, at a concentration that yields therapeutic VPA levels, sensitizes to APAP-mediated hepatotoxicity through the induction of an ER stress–mediated STARD1 upregulation, which promotes mitochondrial cholesterol loading and mitochondrial glutathione deletion.

Our data indicate that VPA+APAP resulted in an early generation of NAPQI-protein adduct formation, a key event involved in APAP-mediated hepatotoxicity, which paralleled the profound depletion of glutathione levels by VPA+APAP in nonfasted mice. While treatment with VPA or APAP alone in nonfasted mice was insufficient to accumulate NAPQI-protein adducts, both drugs caused an early and transient depletion of glutathione, which increased afterward. These data suggest that in nonfasting conditions. the generation of

Figure 4. TUDCA prevents VPA+APAP-induced ER stress and hepatotoxicity in nonfasted mice. (*A*) Western blot of ER stress markers from nonfasted mice given VPA+APAP with or without TUDCA treatment for 4 hours. Control (n = 4 mice), TUDCA (n = 4 mice), VPA+APAP (n = 4 mice), VPA+APAP+TUDCA (n = 4 mice). (*B*) CHOP expression in liver sections on nonfasted mice 24 hours posttreatment with VPA+APAP with or without TUDCA administration. Scale bar: 100 μm. (*C*) STARD1 mRNA levels in liver extracts 4 hours post VPA+APAP treatment with or without TUDCA administration. Control (n = 7 mice), TUDCA (n $\geq$ 5 mice), VPA+APAP (n = 11 mice), VPA+APAP+TUDCA (n = mice). (*D*) STARD1 protein levels in liver extracts 4 hours posttreatment as in (*C*), n = 4 mice/per group. (*E*) Immunohistochemistry analysis of STARD1 examined 24 hours post VPA+APAP treatment with or without TUDCA administration. Scale bar: 100 μm. (*F*) Total and mitochondrial glutathione (GSH) levels from mice treated with VPA+APAP with or without TUDCA. Control (n = 7 mice), TUDCA (n = 5 mice), VPA+APAP (n = 8 mice), VPA+APAP+TUDCA (n = 5 mice). (*G*, *H*) H&E analyses and transaminases from mice 24 hours after treatment with VPA+APAP with or without TUDCA. Control (n = 5 mice), TUDCA (n = 5 mice), VPA+APAP (n = 16 mice), VPA+APAP+TUDCA (n = 7 mice). Scale bar: 100 μm. *$P < .05$ as indicated.

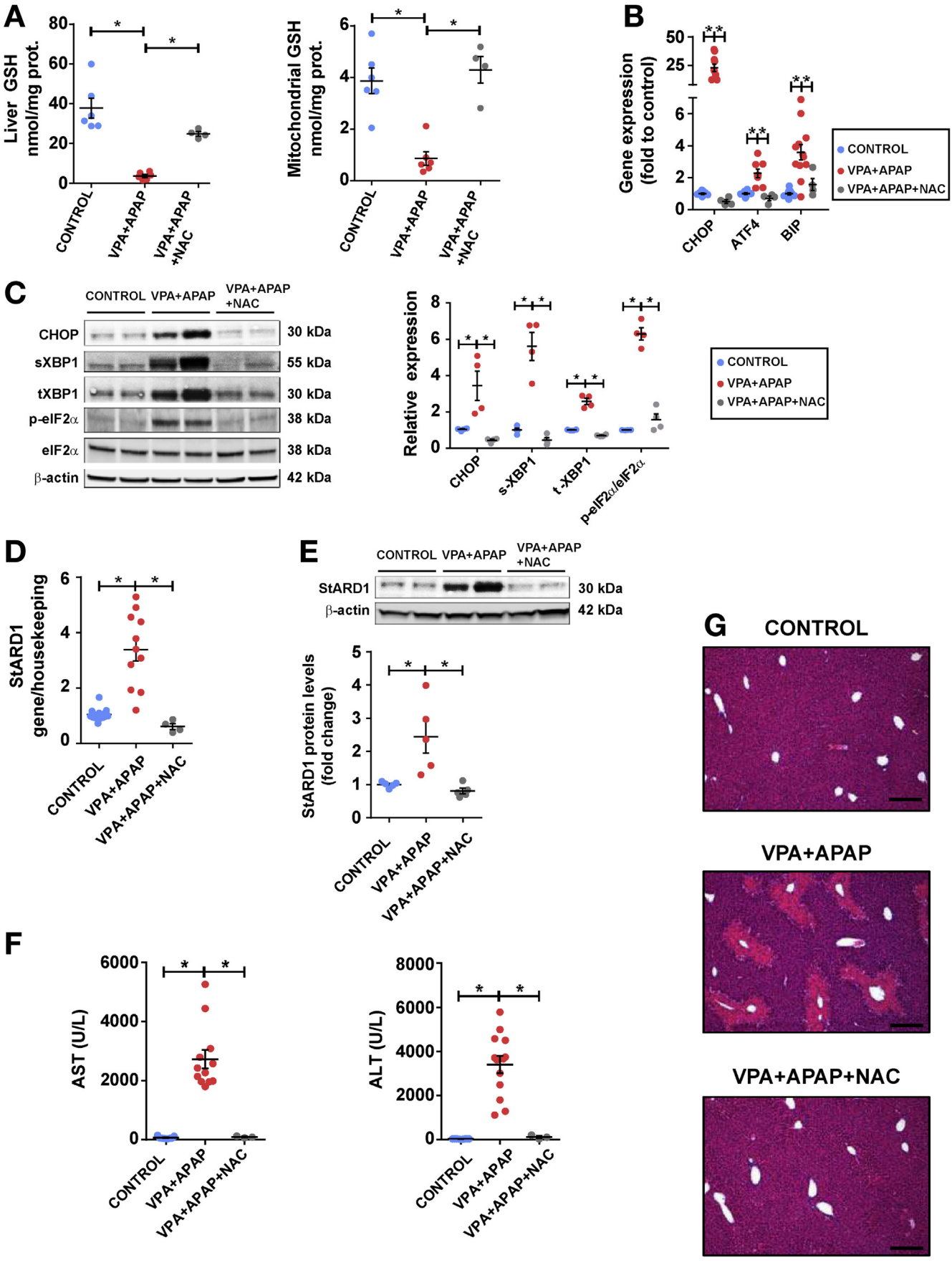
A
Liver GSH nmol/mg prot.
80
60
40
20
0
CONTROL
VPA+APAP
VPA+APAP +NAC
Mitochondrial GSH nmol/mg prot.
6
4
2
0
B
Gene expression (fold to control)
50
25
6
4
2
0
CHOP
ATF4
BIP
CONTROL
VPA+APAP
VPA+APAP+NAC
C
CONTROL VPA+APAP VPA+APAP +NAC
CHOP 30 kDa
sXBP1 55 kDa
tXBP1 30 kDa
p-eIF2α 38 kDa
eIF2α 38 kDa
β-actin 42 kDa
Relative expression
8
6
4
2
0
CHOP
s-XBP1
t-XBP1
p-eIF2α/eIF2α
CONTROL
VPA+APAP
VPA+APAP+NAC
D
StARD1 gene/housekeeping
6
4
2
0
CONTROL
VPA+APAP
VPA+APAP+NAC
E
CONTROL VPA+APAP VPA+APAP +NAC
StARD1 30 kDa
β-actin 42 kDa
StARD1 protein levels (fold change)
5
4
3
2
1
0
CONTROL
VPA+APAP
VPA+APAP+NAC
F
AST (U/L)
6000
4000
2000
0
CONTROL
VPA+APAP
VPA+APAP+NAC
ALT (U/L)
8000
6000
4000
2000
0
CONTROL
VPA+APAP
VPA+APAP+NAC
G
CONTROL
VPA+APAP
VPA+APAP+NAC

NAPQI from APAP is metabolized at the expense of glutathione stores, implying the existence of a sufficient glutathione reservoir or unrestricted capacity for glutathione neosynthesis to conjugate NAPQI to prevent the NAPQI-protein adduct formation. In line with this scenario, we observed that VPA+APAP administration induced the upregulation of CYP2E1 compared with either drug alone, suggesting that the metabolism of APAP into NAPQI following VPA dosing occurs at a rate that may overwhelm the ability of glutathione to form nontoxic mercapturic conjugates. Thus, the generation of NAPQI by the combination of VPA+APAP, but not by VPA or APAP alone, may trigger subsequent downstream events leading to hepatotoxicity in nonfasted mice.

Although all quinones can generate reactive oxygen species through redox cycling, partially substituted quinones also undergo arylation and Michael adduct formation, yielding covalent bonds with nucleophiles, such as cysteinyl thiols. The reported cytotoxicity of arylating quinones correlates with their ability to induce ER stress.[47] As a partially substituted quinone, the affinity of NAPQI to form Michael adducts with protein thiols can account for the ability of VPA+APAP to induce ER stress. Although we did not examine the identity of the NAPQI-protein adducts or their intracellular site of generation following VPA+APAP, it is conceivable that NAPQI may have formed Michael adducts with ER proteins to underlie the observed ER stress, as well as the covalent binding with intramitochondrial proteins, which are known to be a major target of APAP metabolism.[7,8] In addition to forming Michael protein adducts in the ER, the correct protein folding in the ER requires appropriate redox environment, matched by an appropriate glutathione homeostasis. As ER stress can be regulated by antioxidants and glutathione replenishment,[49] the ability of NAPQI to deplete glutathione levels may secondarily contribute to the onset of ER stress caused by VPA+APAP treatment, in parallel with the outcome observed in PMHs. In line with this scenario, we observe that NAC prevents the induction of ER stress by VPA+APAP. In addition to the presence of its nucleophilic thiol, which could directly target NAPQI-protein adducts, NAC is a precursor of glutathione, stimulating its synthesis by providing the rate-limiting cysteine precursor, and therefore it is conceivable that the protective effect of NAC in VPA+APAP hepatotoxicity may imply a dual mechanism involving the prevention of NAQPI-protein adduct formation and glutathione replenishment, thereby abolishing the onset of ER stress, consistent with recent findings in fasted mice treated with APAP.[50] The relevance of the ER stress in the hepatotoxicity caused by VPA+APAP in nonfasted mice is further demonstrated by the time-dependent sequence of events, in which the onset of ER stress by VPA+APAP preceded liver injury, and by the ability of the chemical chaperone TUDCA to abolish the induction of ER stress markers and protect against VPA+APAP-mediated liver injury. Interestingly, both NAC and TUDCA prevented the upregulation of STARD1 by VPA+APAP, consistent with the causal role of ER stress in inducing STARD1 overexpression, underlying a previously unrecognized ER stress-STARD1 axis in APAP hepatotoxicity.

The importance of the induction of STARD1 in the VPA+APAP hepatotoxicity in nonfasted mice is illustrated by the resistance of STARD1$^{\Delta Hep}$ mice to VPA+APAP-induced liver injury, with similar findings observed in fasted STARD1$^{\Delta Hep}$ mice after APAP administration, indicating that STARD1 contributes to APAP hepatotoxicity regardless of the sensitization approach (VPA pretreatment or fasting). Importantly, this outcome is reproduced upon the genetic knockdown of STARD1 in adult wild-type mice, discarding the involvement of compensatory effects in the protection of STARD1$^{\Delta Hep}$ mice against VPA+APAP-induced liver damage. Quite interestingly, nonfasted Sab$^{\Delta Hep}$ mice were equally resistant to VPA+APAP hepatoxicity. These findings complement previous observations in fasted Sab$^{\Delta Hep}$ mice given APAP[10,11] and, consistent with its role as a docking protein for the translocation of phosphorylated JNK to mitochondria, indicate that Sab is a crucial player in APAP-mediated liver injury regardless of the approach of sensitization. Remarkably, our findings in JNK1+2$^{\Delta Hep}$ mice indicate that VPA sensitization to APAP hepatotoxicity in nonfasted mice required hepatocyte JNK1+2 activation, which is in line with previous findings of APAP hepatotoxicity in fasted mice (reviewed in Han et al[11]), but it contrasts with recent findings reporting exacerbated APAP hepatotoxicity in mice with hepatocyte-specific *Jnk1* deletion and global *Jnk2* ablation.[51] Although further work will be required to address this discrepancy, the approach for the genetic deletion of *Jnk1* and *Jnk2* between Cubero et al[51] and our current study was different. Although we deleted *Jnk1* and *Jnk2* selectively in hepatocytes in adult mice by AAV8.TBG.Cre injection, Cubero et al[51] used mice with germ-line deletion of *Jnk1* in hepatocytes and global *Jnk2* knockout, which could lead to the impairment of the developmental protective mechanisms of JNK. Nevertheless, an intriguing finding from our study is the preservation for increased translocation of p-JNK in mitochondrial fractions from STARD1$^{\Delta Hep}$ mice treated with APAP, which suggests a functional interplay

Figure 5. NAC restores glutathione (GSH) levels and prevents VPA+APAP-induced ER stress and STARD1 induction in nonfasted mice. (*A*) GSH levels in liver extracts and mitochondrial fraction from nonfasted given VPA+APAP for 4 hours with or without NAC treatment. Control (n = 5 mice), VPA+APAP (n = 6 mice), VPA+APAP+NAC (n = 4 mice). (*B*, *C*) Expression of ER stress markers in liver extracts of mice given VPA+APAP for 4 hours with or without NAC. Control (n = 4 mice), VPA+APAP (n = 4 mice), VPA+APAP+NAC (n = 4 mice). (*D*, *E*) STARD1 expression following VPA+APAP treatment for 4 hours with or without NAC administration. Control (n = 13 mice), VPA+APAP (n = 11 mice), VPA+APAP+NAC (n = 5 mice). (*F*, *G*) Serum transaminases and H&E analyses of VPA+APAP-treated mice (24 hours) with or without NAC administration. Control (n = 10 mice), VPA+APAP (n = 12 mice), VPA+APAP+NAC (n = 5 mice). Scale bar: 100 μm. *$P < .05$ as indicated.

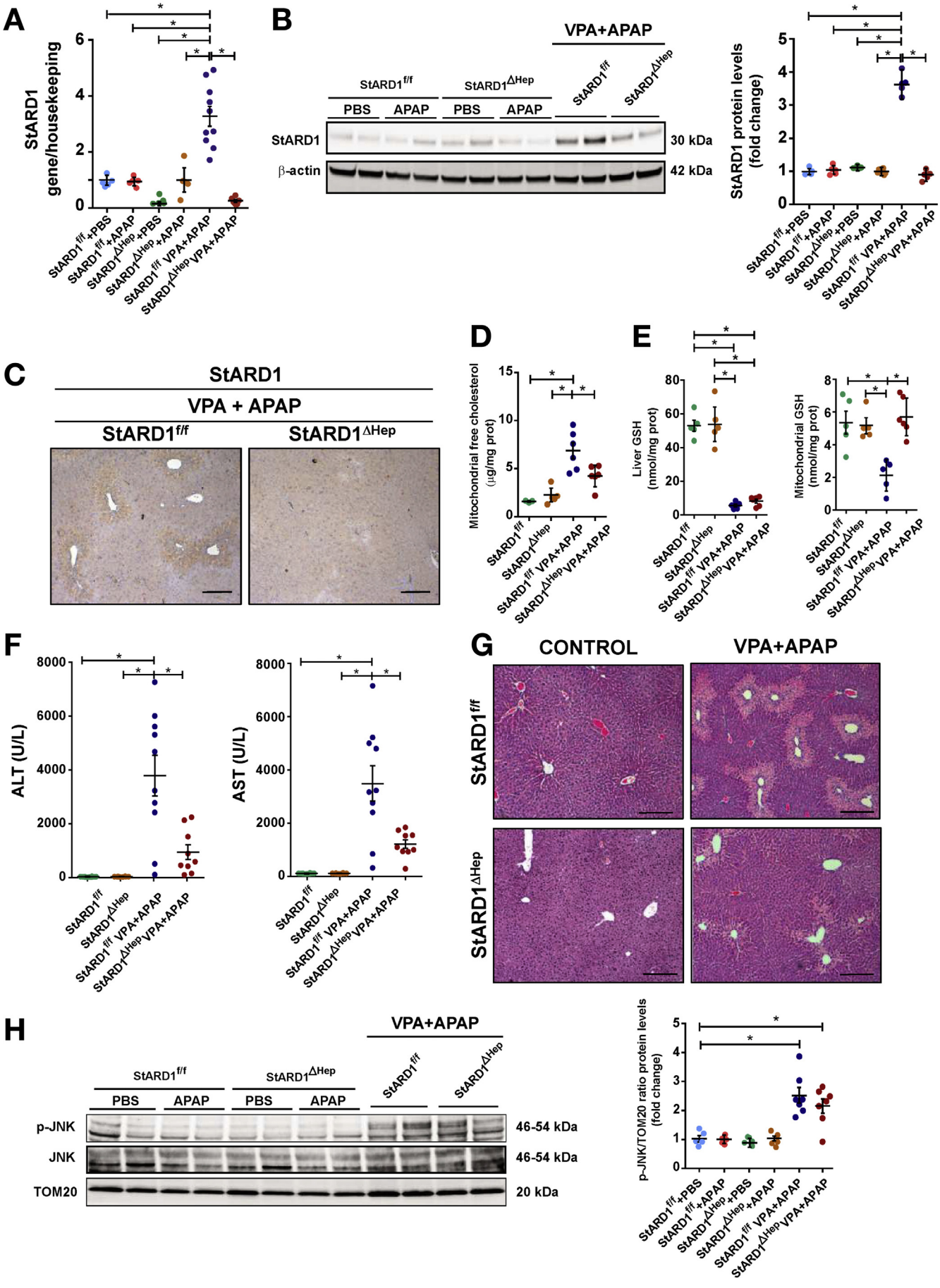
A
StARD1 gene/housekeeping
StARD1f/f+PBS
StARD1f/f+APAP
StARD1ΔHep+PBS
StARD1ΔHep+APAP
StARD1f/f VPA+APAP
StARD1ΔHep VPA+APAP
B
VPA+APAP
StARD1f/f
StARD1ΔHep
PBS
APAP
PBS
APAP
StARD1f/f
StARD1ΔHep
StARD1
β-actin
30 kDa
42 kDa
StARD1 protein levels (fold change)
C
StARD1
VPA + APAP
StARD1f/f
StARD1ΔHep
D
Mitochondrial free cholesterol (μg/mg prot)
E
Liver GSH (nmol/mg prot)
Mitochondrial GSH (nmol/mg prot)
F
ALT (U/L)
AST (U/L)
G
CONTROL
VPA+APAP
StARD1f/f
StARD1ΔHep
H
VPA+APAP
StARD1f/f
StARD1ΔHep
PBS
APAP
PBS
APAP
StARD1f/f
StARD1ΔHep
p-JNK
JNK
TOM20
46-54 kDa
46-54 kDa
20 kDa
p-JNK/TOM20 ratio protein levels (fold change)

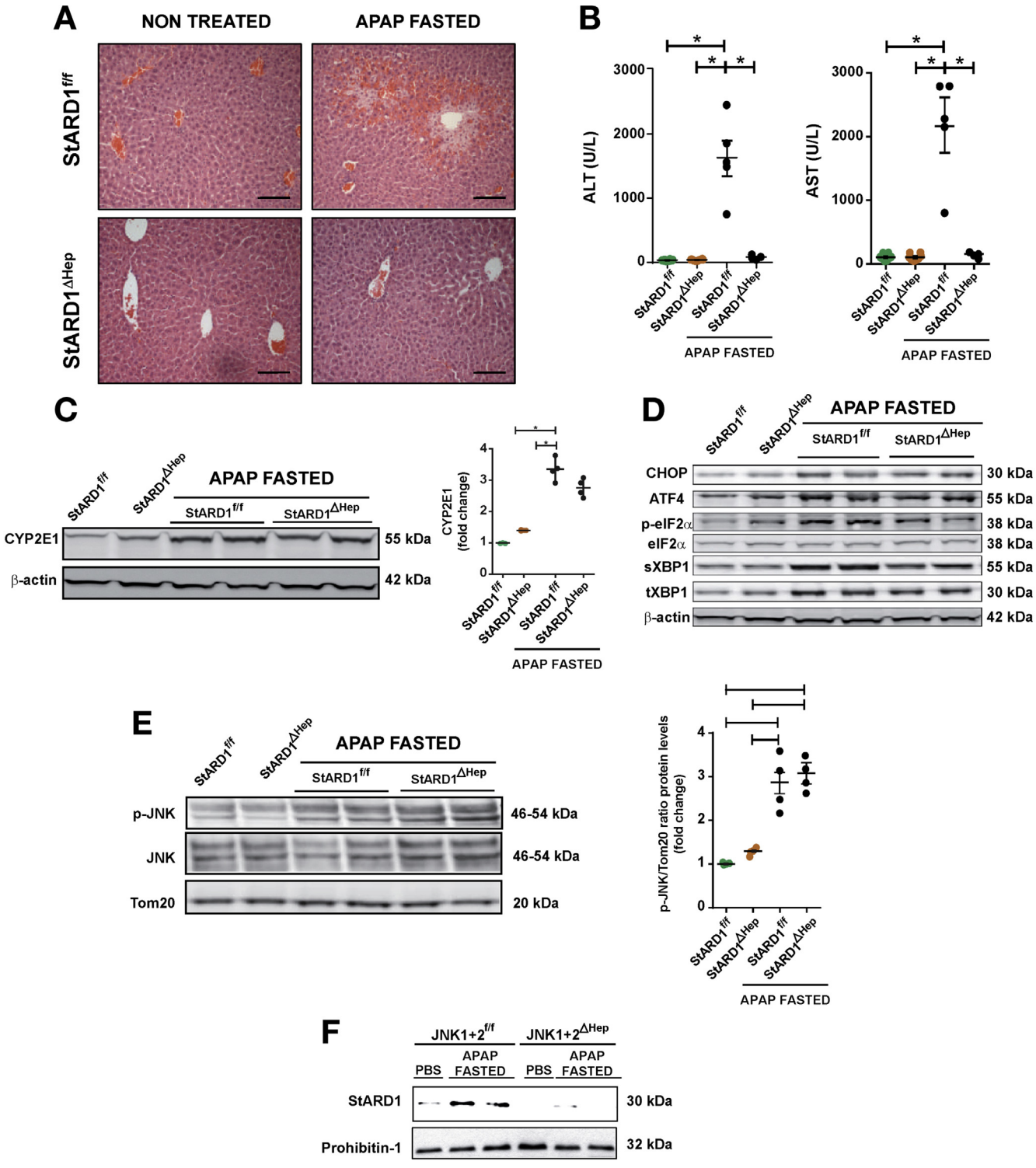

Figure 6. STARD1$^{\Delta Hep}$ mice are resistant to VPA+APAP-induced liver injury. (*A*, *B*) STARD1 expression in STARD1$^{f/f}$ mice ($n \geq 5$) and STARD1$^{\Delta Hep}$ mice ($n \geq 5$) given VPA+APAP (400 mg/kg 3 times 7/12 hours+300 mg/kg) for 6 hours. (*C*) STARD1 expression in liver sections from STARD1$^{f/f}$ and STARD1$^{\Delta Hep}$ mice 24 hours after treatment with VPA+APAP. Scale bar in (*C*) 100 μm. (*D*) Mitochondrial cholesterol in STARD1$^{f/f}$ mice ($n = 6$) and STARD1$^{\Delta Hep}$ mice ($n = 6$) 6 hours after treatment with VPA+APAP. (*E*) Total glutathione (GSH) and mitochondrial GSH levels in STARD1$^{f/f}$ mice ($n = 6$) and STARD1$^{\Delta Hep}$ mice ($n = 6$) 6 hours after treatment with or without VPA+APAP. (*F*, *G*) Serum transaminases and H&E analyses in STARD1$^{f/f}$ mice ($n \geq 8$) and STARD1$^{\Delta Hep}$ mice ($n \geq 8$) 24 hours after treatment with or without VPA+APAP. Scale bar: 100 μm. (*H*) Levels of phosphorylated JNK in mitochondrial fractions from STARD1$^{f/f}$ mice ($n \geq 5$) and STARD1$^{\Delta Hep}$ mice ($n \geq 5$) treated with VPA+APAP for 4 hours. *$P < .05$ as indicated.

between STARD1 and p-JNK to elicit liver injury. This interplay seems to be exerted at least at 2 levels: (1) JNK is required for STARD1 expression, possibly through the induction of ER stress; (2) the role of mitochondrial JNK activation in APAP hepatotoxicity is dependent on STARD1. Extensive further research will be required to elucidate the complementary roles of STARD1 and activated JNK in APAP hepatotoxicity, particularly the elucidation of the mechanisms downstream of JNK involved in the induction of ER stress and subsequent STARD1 activation and how STARD1 sets the adequate physico-chemical scenario in mitochondria for JNK to execute its action in mitochondrial function and liver damage.

To explore the potential relevance of the preceding findings, we investigated the sensitivity of FRGN mice with humanized liver to VPA+APAP and observed that the sensitization by VPA to APAP-mediated hepatotoxicity was recapitulated in vivo in HHs that repopulated the liver of the FRGN mice, as revealed by colocalization of FAH and TUNEL staining. Thus, whereas VPA+APAP induced a cell autonomous toxic effect of human hepatocytes from FRGN mice, the degree of liver injury in the humanized FRGN mice estimated by the release of serum ALT was lower compared with wild-type mice, similar to previous reports in uPA$^{+/+}$/SCID mice repopulated with human hepatocytes.[52] This outcome may reflect a putative functional immaturity of the repopulating HHs or the lack of additional factors involved in APAP hepatotoxicity in the liver of humanized FRGN mice, such as inflammatory cells (eg, macrophages or neutrophils). Whether the reconstitution of human hematopoietic cells in the FRGN mice from transplanted human CD34 stem cells[48] will increase the degree of hepatotoxicity induced by VPA+APAP remains to be investigated.

Finally, we speculate that our findings may have implications in patients with chronic liver disease. There is growing evidence that nonalcoholic fatty liver disease can increase the risk and/or the severity of liver injury induced by different drugs, including APAP.[53] Quite interestingly, we have previously reported that patients with nonalcoholic steatohepatitis exhibit increased expression of STARD1,[54] suggesting that a subset of patients with advanced nonalcoholic fatty liver disease and enhanced free cholesterol content and STARD1 expression may develop liver injury on APAP consumption.

Supplementary Material

Note: To access the supplementary material accompanying this article, visit the online version of *Gastroenterology* at www.gastrojournal.org, and at https://doi.org/10.1053/j.gastro.2019.04.023.

References

1. Lee WM. Drug-induced acute liver failure. Clin Liver Dis 2013;17:575–586.
2. Kaplowitz N. Idiosincratic drug hepatotoxicity. Nat Rev Drug Discovery 2005;4:489–499.
3. Reuben A, Tillman H, Fontana RJ, et al. Outcomes in adults with acute liver failure between 1998 and 2013: an observational cohort study. Ann Intern Med 2016;164:724–732.
4. Kullack-Ublick GA, Andrade RJ, Merz M, et al. Drug-induced liver injury: recent advancs in diagnosis and risk assessment. Gut 2017;66:1154–1164.
5. Watkins PB, Kaplowitz N, Slattery JT, et al. Aminotransferase elevations in healthy adults receiving 4 grams of acetaminophen daily: a randomized controlled trial. JAMA 2006;296:87–93.
6. Mitchell JR, Jollow DJ, Potter WZ, et al. Acetaminophen-induced hepatic necrosis. IV. Protective role of glutathione. J Pharmacol Exp Ther 1973;187:211–217.
7. Yuan L, Kaplowitz N. Mechanisms of drug-induced liver injury. Clin Liver Dis 2013;17:507–518.
8. Jaeschke H, Bajt ML. Intracellular signaling mechanisms of acetaminophen-induced liver cell death. Toxicol Sci 2006;89:31–41.
9. Moles A, Torres A, Baulies A, et al. Mitochondrial-lysosomal axis in acetaminophen hepatotoxicity. Front Pharmacol 2018;9:453.
10. Win S, Than TA, Min RW, et al. c-Jun N-terminal kinase mediates mouse liver injury through a novel Sab (SH3BP5)-dependent pathway leading to inactivation of intramitochondrial Src. Hepatology 2016;63:1987–2003.
11. Han D, Dara L, Win S, et al. Regulation of drug-induced liver injury by signal transduction pathways: critical role of mitochondria. Trends Phamacol Sci 2013;34:243–253.
12. Jaescke H. Mechanisms of acetaminophen hepatotoxicity: do we need JNK for cell death? Gastroenterology 2016;151:371–372.
13. Zhao M, Zhang T, Li G, et al. Associations of CYP2C9 and CYP2A6 polymorphisms with the concentrations of valproate and its hepatotoxin metabolites and valproate-induced hepatotoxicity. Basic Clin Pharmacol Toxicol 2017;121:138–143.
14. Farinelli E, Giampaoli D, Cenciarini A, et al. Valproic acid and nonalcoholic fatty liver disease: a possible association? World J Hepatol 2015;28:1251–1257.
15. Verrotti A, Manco R, Agostinelli S, et al. The metabolic syndrome in overweight epileptic patients treated with valproic acid. Epilepsia 2009;51:268–273.
16. Lheureux PE, Hantson P. Carnitine in the treatment of valproic acid-induced toxicity. Clin Toxicol 2009;47:101–111.

Figure 7. Fasted STARD1$^{\Delta Hep}$ mice are protected against APAP hepatotoxicity. (*A*, *B*) Representative H&E analyses and serum transaminases of overnight fasted STARD1$^{f/f}$ (n = 5) and STARD1$^{\Delta Hep}$ (n = 5) mice 24 hours after treatment with APAP (300 mg/kg). (*C*) CYP2E1 expression from fasted STARD1$^{f/f}$ (n = 4) and STARD1$^{\Delta Hep}$ (n = 4) mice 2 hous after treatment with APAP. (*D*) ER stress markers from fasted STARD1$^{f/f}$ and STARD1$^{\Delta Hep}$ mice 4 hours after treatment with APAP. (*E*) Mitochondrial p-JNK levels from fasted STARD1$^{f/f}$ (n = 4) and STARD1$^{\Delta Hep}$ (n = 4) mice 4 hous after treatment with APAP. (*F*) STARD1 in mitochondrial fraction from fasted JNK1+2$^{\Delta Hep}$ mice 4 hours after APAP (n = 3). Results are the mean ± standard error of the mean of 3 to 5 mice. *$P < .05$ as indicated.

17. Tong V, Teng XW, Chang TK, et al. Valproic acid II: effects on oxidative stress, mitochondrial membrane potential and cytotoxicity in glutathione-depleted rat hepatocytes. Toxicol Sci 2005;86:436–443.
18. Spahr L, Negro F, Rubbia-Brandt L, et al. Acute valproate-associated microvesicular steatosis: could the [13C]methionine breath test be useful to assess liver mitochondrial function? Dig Dis Sci 2001;46:2758–2761.
19. Cengiz M, Yüksel A, Seven M. The effects of carbamazepine and valproic acid o the erythrocyte glutathione, glutathione peroxidase, superoxide dismutase and serum lipid peroxidation in epileptic children. Pharmacol Res 2000;41:423–425.
20. Hurd RW, Van Rinsvelt HA, Wilder BJ, et al. Selenium, zinc and copper changes with valproic acid:possible relation to drug side effects. Neurology 1984;34:1393–1395.
21. Brookes RL, Crichton S, Wolfe CDA, et al. Sodium valproate, a histone deacetylase inhibitor, is associated with reduced stroke risk after previous ischemic stroke or transient ischemic attack. Stroke 2018;49:54–61.
22. Zhang C, Liu S, Yuan X, et al. Valproic acid promotes human glioma u87 cells apoptosis and inhibits glycogen synthase kinase-3β through ERK/Akt signaling. Cell Physiol Biochem 2016;39:2173–2185.
23. Palsamy P, Bidasee KR, Shinohara T. Valproic acid suppresses Nrf2/Keap1 dependent antioxidant protection through induction of endoplasmic reticulum stress and Keap1 promoter DNA demethylation in human lens epithelial cells. Exp Eye Res 2014;121:26–34.
24. Segar KP, Chandrawanshi V, Mehra S. Activation of unfolded protein response pathway is important for valproic acid mediated increase in immunoglobulin G productivity in recombinant chinese hámster ovary cells. J Biosci Bioenerg 2017;124:459–468.
25. Li Z, Wu F, Zhang X, et al. Valproate attenuates endoplasmic reticulum stress-induced apoptosis in SH-SY5Y cells via the AKT/GSK3b signaling pathway. Int J Mol Sci 2017;8:18.
26. McAlpine CS, Bowes AJ, Khan MI, et al. Endoplasmic reticulum stress and glycogen synthase kinase 3b activation in apolipoproteinE-deficient mouse models of accelerated aterosclerosis. Artherioscler Thromb Vasc Biol 2012;32:82–91.
27. Nelson-DeGrave VL, Wickenheisser JK, Cockrell JE, et al. Valproate potentiates androgen biosynthesis in human ovarian theca cells. Endocrinology 2004;145:799–808.
28. Brion L, Gorostizaga A, Gómez NV, et al. Valproic acid alters mitochondrial cholesterol transport in Y1 adrenocortical cells. Toxicol In Vitro 2011;25:7–12.
29. Miller W, Bose HS. Early step in steroidogenesis:intracelular cholesterol trafficking. J Lipid Res 2011;52:2111–2135.
30. **Fernandez A**, **Colell A**, Caballero F, et al. Mitochondrial S-adenosyl-L-methionine transport is insensitive to alcohol-mediated changes in membrane dynamics. Alcohol Clin Exp Res 2009;33:1169–1180.
31. **Marí M**, **Caballero F**, Colell A, et al. Mitochondrial free cholesterol loading sensitizes to TNF- and Fas-mediated steatohepatitis. Cell Metab 2006;4:185–198.
32. Caron KM, Soo SC, Wetsel WC, et al. Targeted disruption of the mouse gene encoding steroidogenic acute regulatory protein provides insights into congenital lipoid adrenal hyperplasia. Proc Natl Acad Sci U S A 1997;94:11540–11545.
33. Azuma H, Paulk N, Ranade A, et al. Robust expansion of human hepatocytes in Fah-/-/Rag2-/-/Il2rg-/- mice. Nat Biotechnol 2007;25:903–910.
34. Dowdell KC, Pesniack L, Hoffmann V, et al. Valproic acid, a histone deacetylase inhibitor diminishes lymphoproliferation in the Fas deficient MRL/lpr-/- murine model of autoinmune lymphoproliferative syndrome. Exp Hematol 2009;37:487–494.
35. Tremolizzo L, Carboni G, Ruzicka WB, et al. An epigenetic mouse model for molecular and behavioral neuropathologies related to schizoprenia vulnerability. Proc Natl Acad Sci U S A 2002;99:17095–17100.
36. Pinder RM, Brogden RN, Speight TM, Avery GS. Sodium valproate: a review of its pharmacological properties and therapeutic efficacy in epilepsy. Drugs 1977;13:81–123.
37. Pessayre D, Dolder A, Artigou JY, et al. Effect of fasting on metabolite-mediated hepatotoxicity in the rat. Gastroenterology 1979;77:264–271.
38. Gujral JS, Knight TR, Fashood A, Bajt ML, Jaeschke H. Mode of cell death after acetaminophen overdose in mice:apoptosis or oncotic necrosis? Toxicol Sci 2002;67:322–328.
39. Arakane F, King SR, Du Y, et al. Phosphorylation of sterodogenic acute regulatory protein (StAR) modulates its activity. J Biol Chem 1997;272:32656–32662.
40. Manna PR, Soh JW, Stocco DM. The involvement of specific PKC isoenzymes in phorbol ester-mediated regulation of steroidogenic acute regulatory protein expression and steroid synthesis in mouse Leydig cells. Endrocrinology 2011;152:313–325.
41. Charman M, Kennedy BE, Osborne N, et al. MLN64 mediates egress of cholesterol from endosomes to mitochondria in the absence of functional Niemann-Pick Type C1 protein. J Lipid Res 2010;51:1023–1234.
42. Balboa E, Castro J, Pinochet MJ, et al. MLN64 induces mitochondrial dysfunction associated with increased mitochondrial cholesterol content. Redox Biol 2017;12:274–284.
43. **Fernandez A**, **Matias N**, Fucho R, et al. ASMase is required for chronic alcohol induced hepatic endoplasmic reticulum stress and mitochondrial cholesterol loading. J Hepatol 2013;59:805–813.
44. Soccio R, Adams R, Maxwell K, et al. Differential gene regulation of StarD4 and StarD5 cholesterol transfer proteins. Activatin of StarD4 by sterol regulatory element-binding protein-2 and StarD5 by endoplasmic reticulum stress. J Biol Chem 2005;280:19410–19418.
45. Rodriguez-Agudo D, Calderon-Dominguez M, Medina MA, et al. ER stress increases StarD5 expression by stabilizing its mRNA and leads to relocalization of its protein from the nucleus to the membranes. J Lipid Res 2012;53:2708–2715.

46. Paz C, Cornejo Maciel F, et al. Role of protein phosphorylation and tyrosine phosphatases in the adrenal regulation of steroid synthesis and mitochondrial function. Front Endocrinol 2016;7:60.
47. Wang X, Thomas B, Sachdeva R, et al. Mechanism of arylating quinone toxicity involving Michael adduct formation and induction of endoplasmic reticulum stress. Proc Natl Acad Sci U S A 2006;103:3604–3609.
48. Wilson EM, Bial J, Tarlow B, et al. Extensive double humanization of both liver and hematopoiesis in FRGN mice. Stem Cell Res 2014;13:404–412.
49. Malhotra JD, Miao H, Zhang K, et al. Antioxidants reduce endoplasmic reticulum stress and improve protein secretion. Proc Natl Acad Sci U S A 2008;105:18525–18530.
50. Paridaens A, Raevens S, Colle I, et al. Combination of tauroursodeoxycholic acid and N-acetylcysteine exceeds standard treatment for acetaminophen intoxication. Liver Int 2016;37:748–756.
51. Cubero FJ, Zoubek ME, Hu W, et al. Combined activities of JNK1 and JNK2 in hepatocytes protect against toxic liver injury. Gastroenterology 2016;150:968–981.
52. Sato Y, Yamada H, Iwasaki K, et al. Human hepatocytes can repopulate mouse liver. Histophatology of the liver in human hepatocyte-transplanted chimeric mice and toxicologic response to acetaminophen. Toxicol Pathol 2008;36:581–591.
53. Massart J, Begriche K, Moreau C, et al. Role of nonalcholic fatty liver as risk factor for drug-induced hepatotoxicity. J Clin Trans Res 2017;3:212–232.
54. Caballero F, Fernandez A, De Lacy AM, et al. Enhanced free cholesterol, SREBP-2 and StAR expression in human NASH. J Hepatol 2009;50:789–796.

Author names in bold designate shared co-first authorship.

Received July 17, 2018. Accepted April 20, 2019.

Reprint requests
Address requests for reprints to: Jose C. Fernández-Checa, MD, Hospital Clinical, Provincial, Barcelona 08036, Spain. e-mail: checa229@yahoo.com or cgrbam@iibb.csic.es; fax: 34-93-363-8310.

Acknowledgments
Author contributions: S.T., A.B., N.I-U., R.F., C.A-V., E.S-V., S.N., D.R., V.R., S.W., and T.A. performed experimental studies and analysis of data; L.W. and M.G. analyzed data from humanized FRGN mice; M.I.L, R.J.A., N.K., C.G.-R,. and J.C.F-Ch. analyzed and discussed data; C.G-R. and J.C.F-Ch. designed and supervised study, discussed data, and drafted the manuscript.

Conflicts of interest
The authors disclose no conflicts.

Funding
We acknowledge the support from grants SAF2014–57674R, SAF-2015–69944R, and SAF2017–85877R from Plan Nacional de I+D, Spain, and by the CIBEREHD; the center grant P50AA011999 Southern California Research Center for ALPD and Cirrhosis funded by National Institute on Alcohol Abuse and Alcoholism/National Institutes of Health (NIH); the NIH R01DK06715 and the USC Research Center for Liver Diseases P30DK485522 Instrumentation (NK), as well as support from AGAUR of the Generalitat de Catalunya SGR-2017–1112, European Cooperation in Science & Technology (COST) ACTION CA17112 Prospective European Drug-Induced Liver Injury Network, and the Fundación BBVA.